bioresources.com

The Effects of Electron Beam Irradiation Dose on the Mechanical Performance of Red Maple (*Acer rubrum*)

Timothy Starr, David P. Harper,* and Timothy G. Rials

To understand how electron beam irradiation affects wood physically and chemically, irradiated maple beams (*Acer rubrum*) and veneers were examined using three-point bend tests, dynamic mechanical analysis (DMA), and NIR- and FTIR- spectroscopy. The MOR from the bending tests revealed a significant decline in the red maple's strength after a dose of 80 kGy. DMA results showed evidence of crosslinking of the amorphous content of the wood at low doses, followed by degradation at higher doses, with the change in response occurring around 80 kGy. Infrared spectroscopy revealed that the components of wood that were most impacted were the phenolic hydroxyl structures of lignin and cellulose hydroxyls, with the greatest effects being seen after 80 kGy.

*Contact information: Center for Renewable Carbon, The University of Tennessee, 2506 Jacob Dr., Knoxville, TN 37996; *Corresponding author: dharper4@utk.edu*

INTRODUCTION

Wood is a remarkably useful and versatile renewable resource, as it is used as structural material, furniture, packaging, and as a feedstock for liquid fuels production. Wood composites, such as plywood, oriented strand board (OSB), and medium density fiberboard (MDF), can be produced in sizes and dimensions that are unavailable from raw lumber. However, despite the many advantages of wood composites, there are significant disadvantages associated with their manufacturing. The temperatures required for thermal curing can be harmful to the wood components. If the moisture content is not carefully monitored, internal stresses can result from the pressure generated by moisture at such high temperatures. During the cool-down phase after curing is complete, thermal shrinkage of the resin can cause delamination at the wood/resin interface due to differences in their thermal expansion coefficients (Singh 2001). Other issues include volatile emissions, time requirements for curing, and size limitations. Probably the biggest concern regarding thermal curing of wood composites is the immense energy requirements, and therefore processing costs.

Radiation curable adhesives present a solution to most, if not all, of these problems. Electron beam radiation, specifically, has been studied extensively as a means of curing composites made from such resins (Singh 2001; Song 2005; Griffith *et al.* 2006). It answers the problem of time requirements by allowing much higher product throughput, it reduces volatile emissions significantly, it allows for the curing of much larger, thicker pieces, and most importantly, it drastically reduces energy requirements (Singh 2001). For example, it has been estimated that radiation vulcanization is 3 to 6 times more energy efficient than thermal vulcanization (Ivanov 1992).

With so many advantages over current thermal curing practices, radiation curing is definitely an alternative that needs to be pursued. However, just like thermal curing, radiation curing has the potential to damage the wood. Thus, the doses in which damage becomes significant needs to be identified. This holds true with other potential applications where the use of ionizing radiation can serve other purposes such as for the phytosanitation of wood packaging (Hallman 2011) and as a pretreatment for production of biofuels (Driscoll *et al.* 2009). In the case of phytosanitation, the goal will be to kill pathogens with minimal damage to the woods mechanical and physical integrity, which is similar to the goal of curing adhesive. Alternatively, pretreatments for biofuels would use ionizing radiation to disrupt the cell wall structure to allow for more efficient bioconversion.

Wood is composed mainly of cellulose (40 to 50% by mass), hemicellulose (25 to 35%), and lignin (18 to 35%), which are three naturally produced polymers (Pettersen 1984). Lignin has a highly variable structure, which lends itself to random amorphous configurations. Cellulose, on the other hand, is highly ordered and is mostly found in tightly packed crystalline conformations, though some semi-crystalline and amorphous regions do exist as well. Research regarding the effect of ionizing radiation on wood has found that lignin is the primary target of the radiation, breaking it down into smaller molecular weight units (Hon and Shang-Tzen 1984). When cellulose is affected, it is primarily in the amorphous regions where the chains are not so tightly packed (Tsuchikawa and Siesler 2003; Mitsui *et al.* 2008). Nevertheless, irradiated cellulose can experience a depolymerization and decrease in crystallinity given a high enough dose; however the limiting dose is dependent on the source (x-ray, e-beam, or gamma), energy, and dose rate (Saeman *et al.* 1952, Khan *et al.* 1986, Despot *et al.* 2012) of irradiation. In a study of the effect of e-beam irradiation on natural kenaf fibers, Han *et al.* (2006) determined that the molecular weight of the cellulose chains was being lowered due to breakage of the glucosidic linkages, which decreased the amount of alpha-cellulose and increased the amount of the beta-cellulose polymorph. Despite this, their infrared studies indicated no notable change in the spectra of the treated and untreated fibers.

The effect of radiation on wood components is not all destructive, however. The ultrastructure of wood exposed to high energy ionizing irradiation dose not display a visible impact until the dose exceeds 1000 kGy (Fengel and Wegener 1989). Many studies have indicated that there is a correlation between cellulose depolymerization and dose (Pruzinec *et al.* 1981; Bouchard *et al.* 2006; Han *et al.* 2006). The Han study of kenaf fibers mentioned previously was conducted with e-beam doses of 100, 200, and 500 kGy. On the other hand, a study of the usage of e-beam for fiber preparation for composite reinforcement concluded that a dose of 10 kGy would be useful in contributing to the strength of the interface between the fibers and the resin (Han *et al.* 2006). Therefore, it is important to determine where in the spectrum of e-beam radiation doses the non-destructive/beneficial behavior end and where the destructive reactions begin for a given beam energy.

EXPERIMENTAL

The present research was based on two studies involving maple wood (*Acer rubrum*) irradiated with a variety of e-beam doses. Red maple was selected as the model species since it is a common hardwood in the Eastern U.S. with a density of 0.54 g/cm^3 at 12% equilibrium moisture content; it has similar density to many underused hardwoods

bioresources.com

(Kretschmann 2010). Maple beams were used in three-point bending tests and were examined with near infrared spectroscopy. Maple veneers were used in dynamic mechanical analysis and were examined with Fourier-transform infrared (FTIR) spectroscopy.

Sample Preparation

Eighty maple beams were prepared measuring 25 mm by 25 mm in cross section and 450 mm long. Sliced maple veneer measuring 0.5 mm thick was cut into 48 strips measuring 9.64 mm in the radial and 50 mm in the longitudinal direction. All samples were conditioned under ambient conditions for a minimum of two weeks. The samples were sent to an electron beam facility at Sterigenics in San Diego, CA, where they received one of the following mean targeted doses of radiation: 0, 5, 10, 20, 40, 80, 120, or 180 kGy. The electron accelerator used was a low power linear accelerator at Sterigenics rated at 12 MeV and 8 kW, with a 6 ms pulse at a pulse rate of 180 Hz. The dose was calibrated by aluminum calorimetry. A block of aluminum was place on the line at a given speed and the temperature rise was measured and correlated to a known dose for that temperature to within an uncertainty of 6% for each sample. Line speed and the number of passes through the e-beam then subsequently controlled the mean total dose to which the sample was subjected. The irradiation dose was split evenly so that each sample was flipped leading to a minimum of two passes to assure the top and bottom was subjected to the same conditions with up to a maximum of 32 kGy/pass. Previous research has demonstrated that the dose to a depth of 4cm is flat for 1 g/cm^3 sample (Purdy *et al.* 2012). Since the density of the wood was less than 1 g/ cm^3, flipping the sample was an extra precautionary measure but largely unnecessary. Dosimetry was not performed on the samples after irradiation, but was targeted based on calibration and lines speed. The average dose was delivered in the following manner:

5 kGy: 2 x 2.5 kGy passes
10 kGy: 2 x 5 kGy passes
20 kGy: 2 x 10 kGy passes
40 kGy: 2 x 20 kGy passes
80 kGy: 2 x 32 kGy passes and 2 x 8 kGy passes
120 kGy: 2 x 32 kGy passes and 2 x 28 kGy passes
180 kGy: 4 x 32 kGy passes and 2 x 26 kGy passes

The impact of fractionation of the delivered dose was not evaluated in this study and was assumed to make no difference in the results. The chosen size of each delivered pass was for the convenience of the facility operator and not considered in the analysis. However, there may be possible differences from receiving the dose at once or over several administered passes, as the latter method would allow for cooling between passes and reduces any differences that result from thermal damage. Receiving the whole dose in a single pass would likely lead to excessive heat that would damage the samples. The final result of sample preparation yielded 10 replicates at each dose for the beams, and six replicates of each dose for the veneers. Subsequently, total mean dose is compared, and dose rate or distribution of how dose was applied was not considered.

Variability in the specimens may be introduced by a dose gradient within the specimens. This was not measured or accounted for during subsequent measurements. The delivered dose at any depth in the material is dependent on elastic and inelastic collisions

---

bioresources.com

in the material (Joy 1995). Nevertheless as previously stated, the penetration depth will greatly exceed that of the irradiated wood material, which should minimize the existence of internal gradients.

Three Point Bend Tests

The three-point bend testing was conducted on an Instron 5567 universal testing machine (Instron, Norwood, MA) according to ASTM Method D143 to provide a look at the physical effect of radiation that is manifested in the Modulus of Elasticity (MOE) and the Modulus of Rupture (MOR). The bending samples were conditioned at 15 °C and 50% RH to 9.7 +/- 0.8% moisture content with no significant difference between irradiation treatments.

NIR Spectroscopy

Near infrared (NIR) spectra were collected on wood surfaces after irradiation with a Labspec Pro fiber optic probe made by Analytical Spectral Devices, Inc. (Boulder, CO) over the 350 – 2500 nm range of wavelengths. Four spectra were collected from each specimen, one from each long side of the beam, with each spectra being composed of the average of 32 sample scans.

Mechanical Analysis

Dynamic mechanical analysis was performed in a Perkin Elmer Diamond DMA (Perkin Elmer Inc., Waltham, MA) using dual cantilever bending mode, employing sinusoidal oscillation at frequencies of 1, 2, 4, 10, and 20 Hz. Temperature scans were conducted from room temperature up to about 170 °C at a scanning rate of 5 °C/min. Because of the presence of residual stress in wood polymers, each sample was run through that temperature range twice, the first time to relieve those stresses, and the second for data collection (Sun *et al.* 2007; Horvath *et al.* 2011).

FTIR Spectroscopy

Mid infrared spectra were collected from the samples using a Perkin Elmer Spectrum One instrument with an attenuated total reflectance (ATR-FTIR) accessory (Perkin Elmer Golden Gate Diamond 45º). Like NIR, ATR-FTIR is a surface technique. Sixteen scans at a resolution of 8 cm^{-1} were taken and averaged from each sample before and after radiation. To minimize the effects the variations of wood may have on the spectra, a simple jig was created to make sure that the samples were scanned on the exact same spot both times. The samples were kept in contact using an anvil that is attached to the ATR stage.

RESULTS AND DISCUSSION

Three Point Bend Tests

Bending tests were performed on the maple beams to determine the effect e-beam radiation would have on the bulk properties of the wood as described by the modulus of elasticity, MOE, and the modulus of rupture, MOR. The MOE results in Fig. 1A show that the elastic modulus was relatively invariable across the full range of radiation doses. The MOR (Fig. 1B) of the maple beams, however, did not go unchanged.
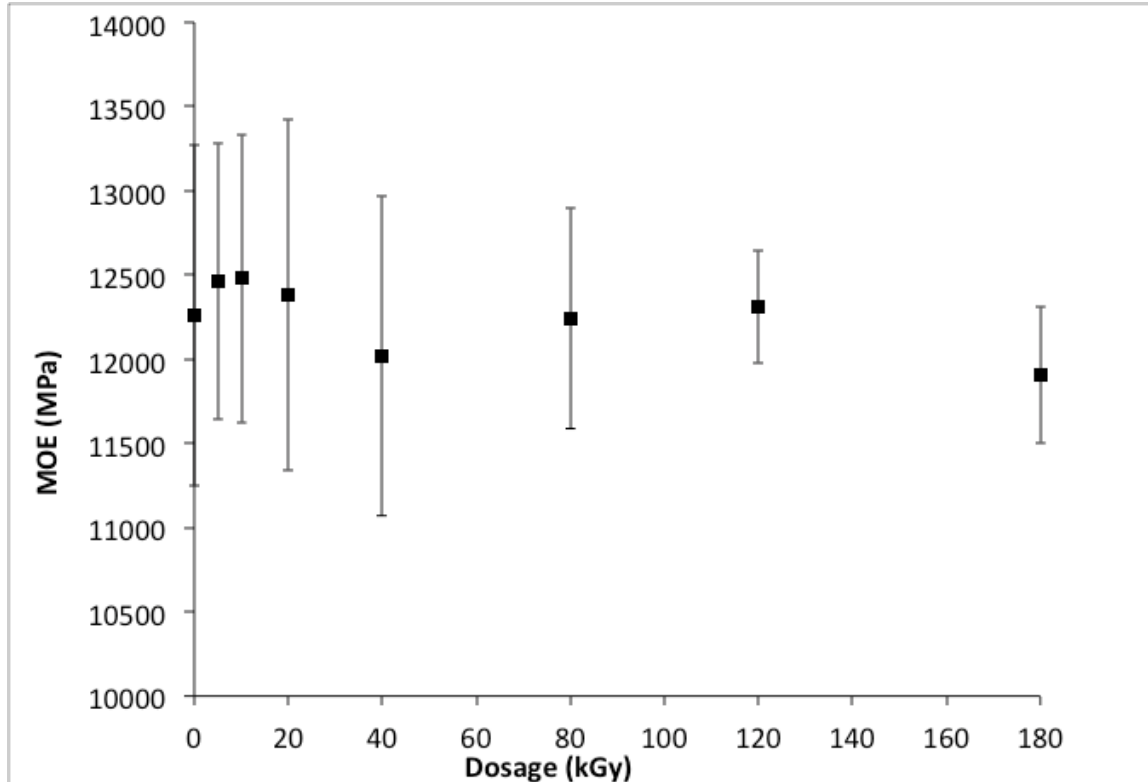
A
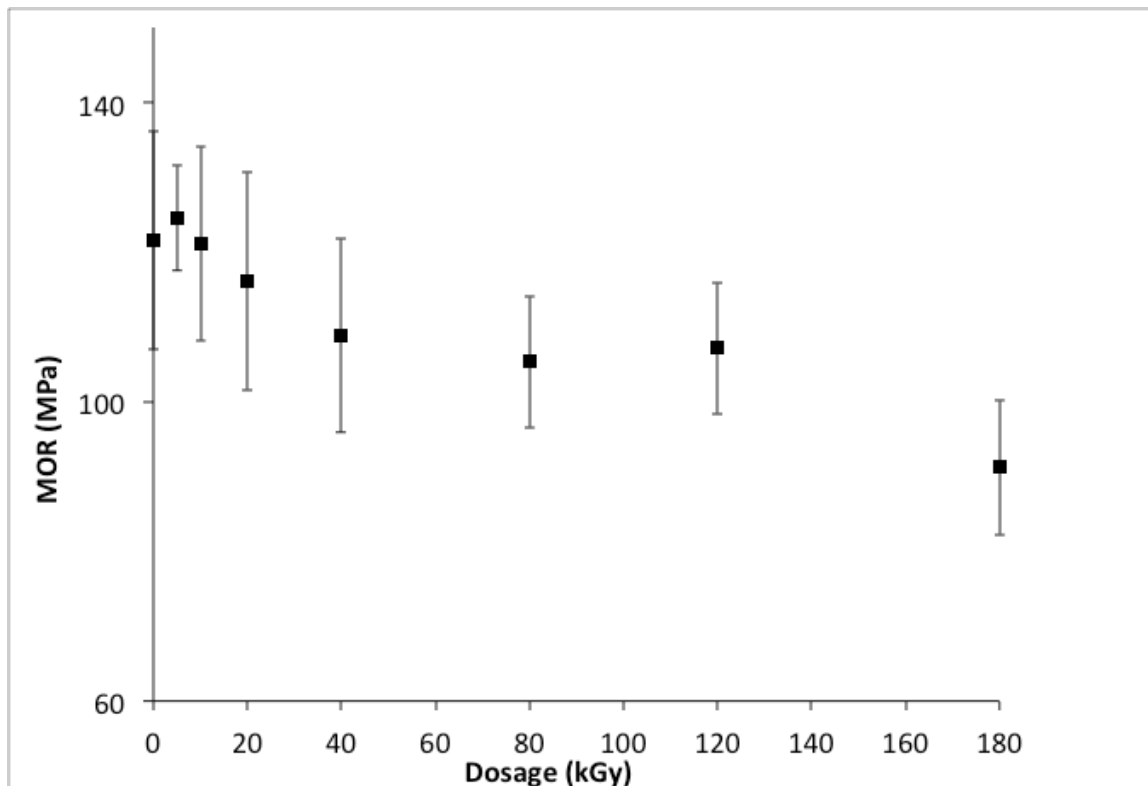
B

Fig. 1. Irradiated maple bending results for (A) modulus of elasticity (MOE) and (B) modulus of rupture (MOR)

bioresources.*com*

Between the two main components in wood, cellulose represents the elastic portion of the material (especially crystalline cellulose) while lignin represents the viscous portion. The lack of change in the elastic modulus suggests that the cellulose was mostly unaffected by the radiation, but the sharp decreases in the MOR, the maximum load-bearing limit, of the wood indicates that something is being affected.

Figure 1B shows that the wood's resistance to fracture decreased with increased radiation dose, with notably sharp reductions in strength between 5 and 40 kGy, and again between 120 and 180 kGy. This trend was also apparent during the execution of the bending tests as the style of failure of the maple beams gradually changed from hairline fractures at low doses to brash failures at high doses, with the 180 kGy specimens having particularly catastrophic failures.

The implication of the bending study is that almost any exposure to e-beam radiation will result in some amount of loss of strength. Only very low doses (< 10kGy) would not show any appreciable difference in strength, but no resin suitable for wood composites could be fully cured with such a low dose (Song 2005). As the radiation dose is increased beyond 5 kGy, there was a steady decrease in MOR until a plateau was reached at 40 kGy. This plateau is a promising result because most e-beam curable resins suitable for wood adhesives, mainly difunctional urethane acrylates and mythacrylates, need up to 40 kGy to reach complete cure (Song 2005). If a higher dose is required to obtain better properties in a wood composite, or if a higher dose is needed because of the electron-scavenging by the wood, that higher dose can be used without sacrificing any more strength in the wood up to a point. Of course, the use of any radiation dose approaching or beyond 120 kGy seems ill-advised because of the further loss of strength.

Dynamic Mechanical Analysis

Dynamic mechanical analysis of the maple veneers yielded many results. First, Fig. 2A shows averaged plots of the storage modulus (E') of the irradiated wood samples as they were heated from room temperature to about 170 ºC. Most of the samples tested between 0 and 120 kGy exhibit similar behavior in E' and were not presented with the exception of the 40 kGy sample (Fig. 2A). For the most part, the E' curves for all doses are grouped closely together, meaning that they exhibit approximately the same stiffness behavior over the tested temperature range. This corresponds with what was observed in the static bending results. Two curves, however, stand out from the group. The 40 kGy curve is noticeably above the rest, indicating that it exhibits overall higher stiffness than the other samples, and the 180 kGy curve is well below the rest implying a lack of stiffness. Since electron beam radiation has the ability to both crosslink and cleave polymer chains, it is possible that crosslinking is going on among the available unsaturated bonds in the polysaccharides and to some lesser extent in lignin, because of its aromatic components up to 40 kGy, after which at higher doses cleavage of existing bonds dominates. Previous work found that degradation initiates at phenolic hydroxyl groups, β-carbons adjacent to α-carbonyl groups, and any conjugated double carbon bonds (Fengel and Wegener 1989). This would explain a slight increase in modulus at 40 kGy, followed by a downward trend in modulus, especially at the 180 kGy dose. Again, it seems that no single trend is responsible for the changes in the physical properties of the wood as the radiation dose increases, and that there are multiple competing events occurring in the chemistry of the wood.
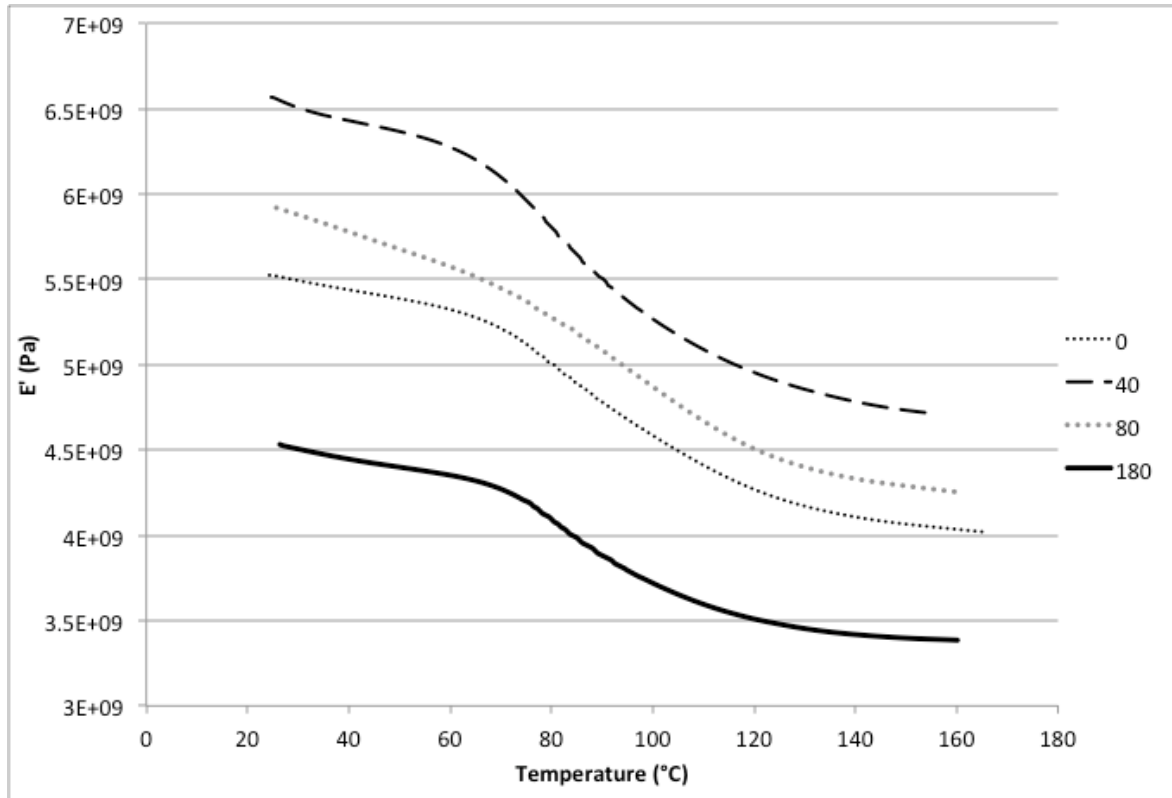
A
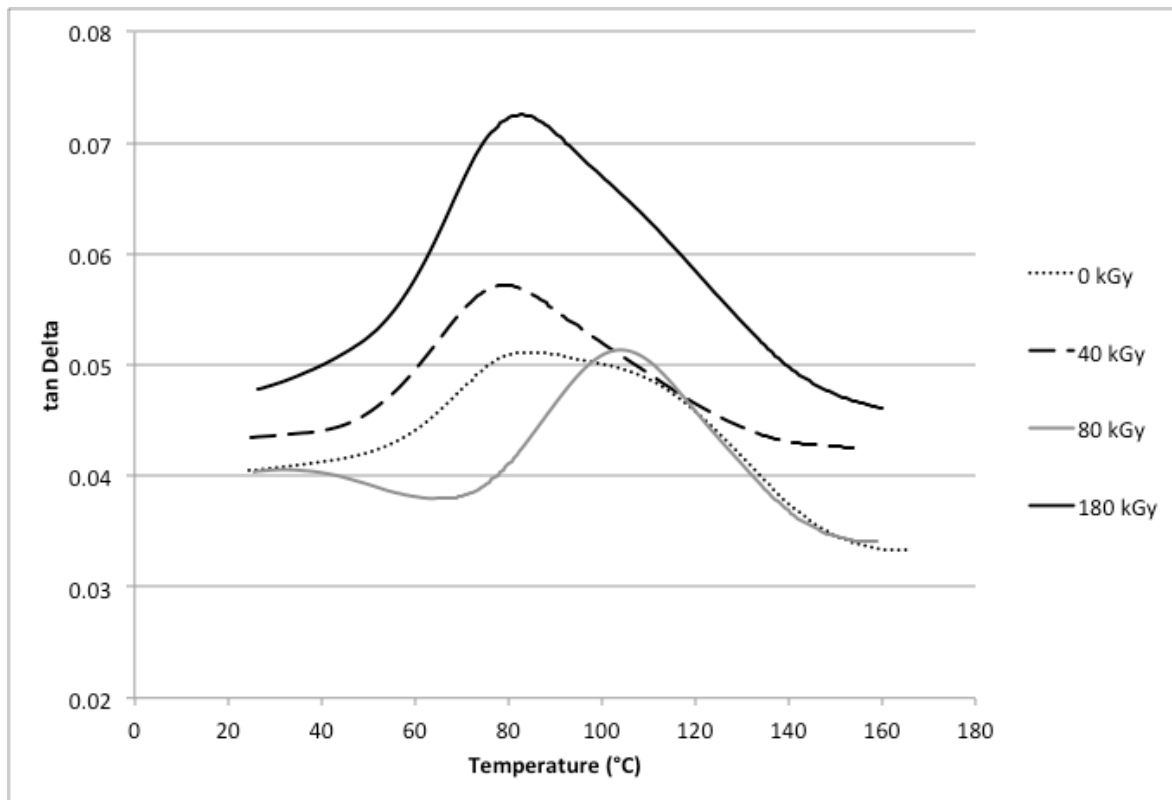
B

Fig. 2. Dynamic mechanical analysis of irradiated maple beams at varying does levels where (A) is the elastic response and (B) is the tan □

Tan δ curves for each dose are shown in Fig. 2B. The value of δ is found during DMA by measuring the phase lag between the applied sinusoidal stress and the resulting oscillating response of the material. Tan δ is the ratio of the loss modulus to the storage modulus, *E"/E'*. The glass transition temperature, T_g, is most commonly defined as the peak of the tan δ curve when testing at a frequency of 1 Hz. T_g was very broad and weak in wood especially at low dose of 0 to 10 kGy, but there was a noticeable shift to higher narrower peaks, indicating a lowering of molecular weight between crosslinks and a trend towards lower temperatures (Fig. 2B). The bimodal nature of the relaxation was reduced at 40 kGy and higher. The T_g values of the irradiated maple veneer samples are shown in Fig. 3A, along with error bars that represent the highs and lows of the averaged replicates. From 0 to 40 kGy, the T_g values varied somewhat, but generally went unchanged. The 80 and 120 kGy samples report much higher T_gs, followed by a dramatic decrease at 180 kGy. This indicates a notable change occurring in the lignin-hemicellulose components, which likely increased crosslinking between 40 and 80 kGy. Change also occurred between 120 and 180 kGy, which likely resulted in a decrease in molecular weight. Once again, the idea of crosslinking at lower doses and commensurate scissioning changes at higher doses seems to be supported by these trends.

In addition to the 1 Hz tan δ plots, which were used to calculate the T_gs, DMA was also performed at 2, 4, 10, and 20 Hz, which reveals a time effect in the glass transition. When the testing is done at higher frequencies, and the stress is being applied faster, the polymer chains do not have as much time to move in response, so the material appears to be less flexible. This results in a shift in the tan δ curve and thus, the T_g. Five different frequencies with five different T_gs gives five pairs of data points that can be used to determine the activation energy required to overcome the glass transition, making use of the Arrhenius equation, $I = I_0 \exp(-E_a/RT)$, where I is the frequency, I_0 is the pre-exponential factor, T is the temperature at the peak of the tan δ curve, and R is the constant 8.314 J/mol·K. Plotting $1/RT$ versus log (I) for every temperature/ frequency pair from a given sample gives a line whose slope is equal to the activation energy, E_a. The E_a values were calculated and averaged among replicates of each radiation dose, and are shown in Fig. 3B. Similar to the T_g plot, the activation energy exhibited little variation between 0 and 40 kGy, and then it spiked sharply at 80 kGy before descending through 120 to 180 kGy. The glass transition involves an expansion of the free volume between polymer chains that allows for more freedom of movement, and the activation energies shown here represent the amount of energy required to allow those movements. Figure 3B indicates that the samples are being crosslinked in the early stages of radiation, peaking at 80 kGy, and then at higher doses the bonds that have been restricting the transition are disappearing.

Infrared Spectroscopy
Near IR

The NIR spectra collected from the maple beams after irradiation were visually indistinguishable when comparing results from the different doses, so Principle Component Analysis (PCA) was used to analyze the spectral data following the method used by Labbé *et al.* (2006). PCA is a mathematical tool that identifies which linear combination of variables out of a multivariate data set are most responsible for the difference between samples, and groups them into principal components (PCs).
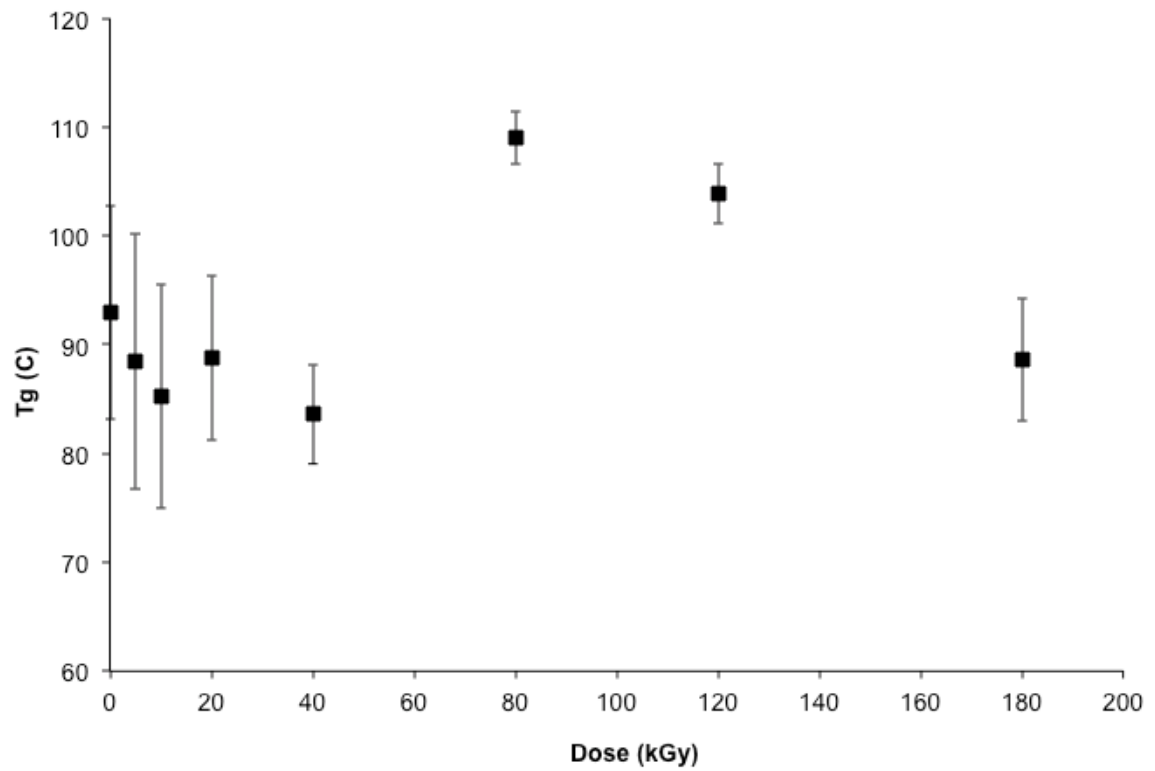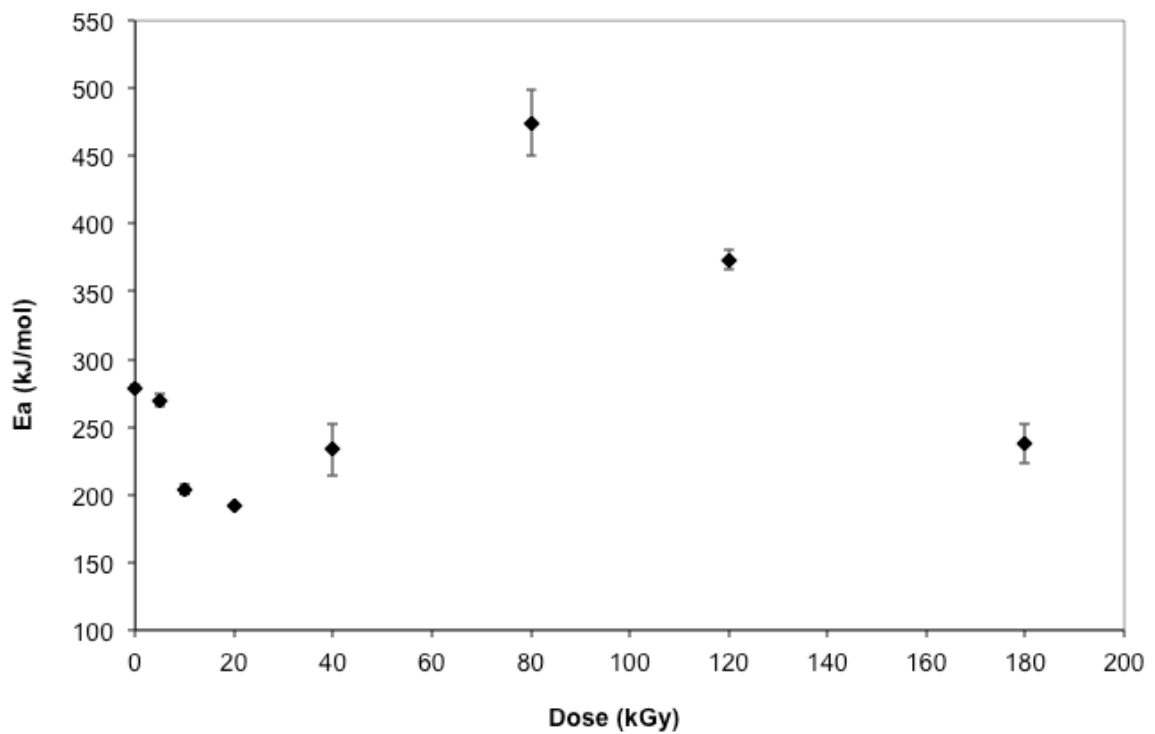
Fig. 3: Changes in the Tg (A) and activation energy (Ea) of the Tg (B) of maple with e-beam dose.

Based on modulus of rupture (MOR) values (Fig. 1A), the sample doses were divided into three groups of similar MOR: High MOR (0 to 20 kGy), Mid MOR (40 to 120 kGY), and Low MOR (180 kGy). PCA performed on the NIR collected from the maple beams shows distinct separations of these three groups, which can be seen in the scores plot in Fig. 4A. Primarily, the 180 kGy samples (Low MOR) are separated from the rest of the samples along PC1, which offers explanation of 65% of the variance among all samples represented. Within the rest of the group, the High and Mid MOR groups are clearly divided along a combination of PCs 1 and 2 (note the diagonal line of separation between the two groups). Based on the PC1 loadings plot in Fig. 4B, the primary contributor to PC 1 is a strong positive band around 1924 nm, which is associated with cellulose hydroxyls (Mitsui *et al.* 2008). Since the High and Mid-MOR groups are positive on PC1 and the Low MOR group is negative on PC1, this means that this peak is decreasing with increasing dose. In other words, the cellulose hydroxyls are being negatively impacted by increasing irradiation. Two notable, but not as strong, negative peaks are apparent in the PC1 loadings: 1632 and 1780 nm, which represent C-H first overtones in lignin and both lignin and cellulose, respectively (Tsuchikawa and Siesler 2003). Their negative loading values indicate that these peaks increase with increasing dose. The defining trends in the NIR study, therefore, were decreasing hydroxyls and increasing C-H first overtones (from both cellulose and lignin) as dose increased. There was no evidence of two separate trends at lower and higher doses. This could be due to the typically exponential response to radiation not being well described by linear approximations in PCA.

FTIR spectroscopy

In addition to NIR spectroscopy, Fourier-Transform spectroscopy was also taken in the Mid IR range (~4000 to 650 cm^{-1}). Of particular interest is the fingerprint region, roughly from 1800 to 800 cm^{-1}, in which the absorption pattern is not just a collection of absorption bands based on the types of bonds present, but rather is the result of interacting vibration patterns generated by the combination of bonds and their arrangements. Much like the NIR spectra, visual evaluation of the ATR-FTIR spectra is not enough to detect changes and trends in the samples as a function of radiation dose, so once again PCA was used to analyze the data.

Data pretreatments were applied to the spectra before analysis. First, multiplicative scatter correction (MSC) was used to remove scatter effects that were produced more by physical characteristics on the surface of the wood than chemical information. Then, each spectrum was normalized by its mean, which causes all spectra to have the same area under the curve, which increases the quantitative significance of each peak. Finally, the variables were averaged by 4 to reduce the noise, and to lighten the computational load.

The PCA results show a very distinct line of demarcation between the low dose (0 – 40 kGy) and high dose (80 – 180 kGy) samples along PC1, as seen in Fig. 5A. According to the loadings plot in Fig. 5B, the key components of PC1 are the peaks at 1592 cm^{-1}, 1059 cm^{-1}, and 1033 cm^{-1} – all with positive loading values, and the peak at 1720 cm^{-1} which has a negative loading value. The peak at 1592 cm^{-1} is due to aromatic skeletal vibrations in lignin (Azadfallah *et al.* 2008), and the peaks at 1059 and 1033 cm^{-1} are from vibrations of the ring structures in cellulose (Kauráková *et al.* 2000). These three, according to PCA, are decreasing with increasing irradiation dose. The peak at 1720 cm^{-1} is assigned to C=O stretching (Colom *et al.* 2003).
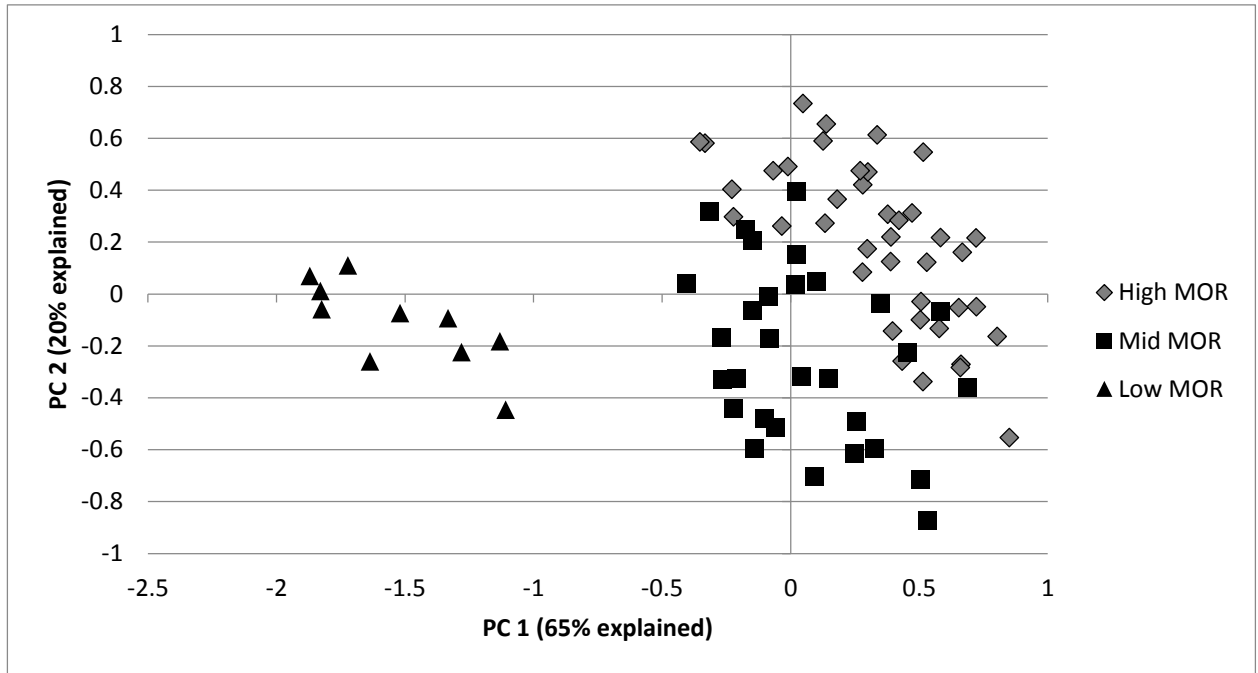
A
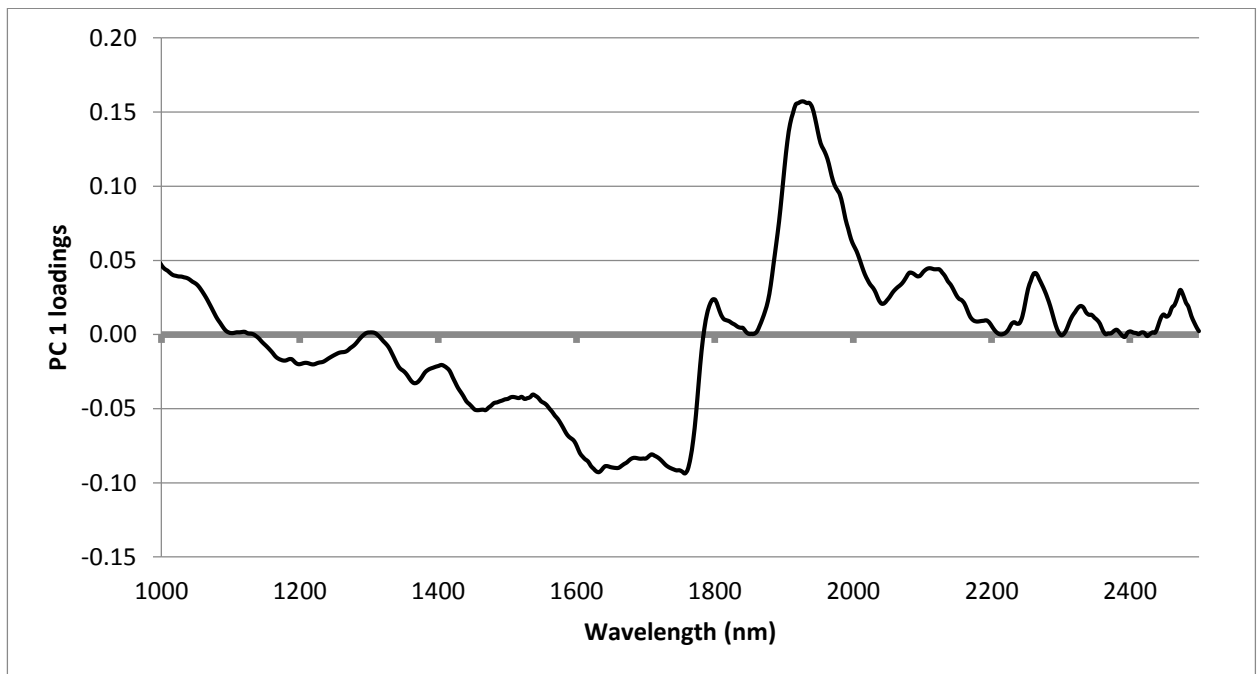
B

Fig. 4. NIR scores plot (A) for PCs 1 and 2 from PCA of irradiated maple beams and loadings plot (B) for PC 1

The NIR study showed that the primary change in the wood as it was irradiated was a decrease in hydroxyls, especially at 180 kGy. According to the ATR-FTIR analysis, carbonyls were increasing, and the aromatics in lignin and the ring structures in cellulose were decreasing as radiation doses increased. Elimination of hydroxyls in cellulose (evident from NIR study) and changes in ring structures (evident in ATR-FTIR study) would negatively impact the strength by reducing hydrogen bonding, which is especially

important in crystalline regions. Any actual chain scissions, which would most likely occur in the amorphous regions of cellulose and lignin would also be main contributors to the loss of strength observed in bending tests.
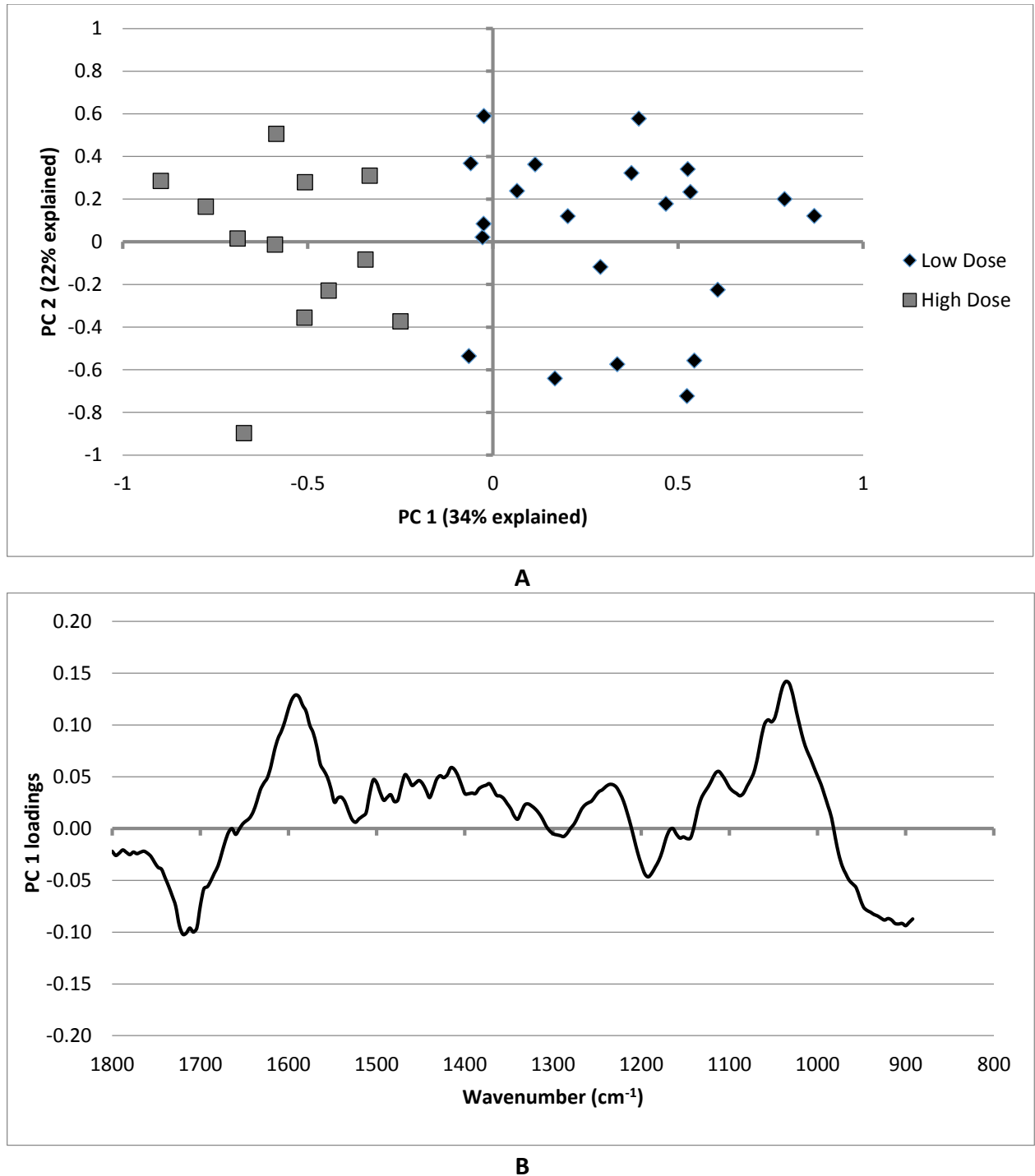
A

B

Fig. 5. PCA scores plot (A) for FTIR of irradiated maple veneers and loadings for PC 1 (B)

CONCLUSIONS

The MOR data from the bending tests suggest that radiation doses for curing of red maple composites be restricted to the plateau between 40 and 80 kGy, beyond which increased dose showed no further decrease in physical performance. The DMA experiments showed a decrease in stiffness between 40 kGy and 180 kGy. This along with the T_g values and the E_a values, which peaked at 80 kGy, seemed to indicate early cross linking at lower doses and chain scission at higher doses. Analysis of the storage modulus, T_g, E_a, and infrared studies all seem to point to 80 kGy as the point at which the most destructive effects start to take place. Therefore, a dose higher than 80 kGy should probably not be used to cure composites. However, doses above 80 kGy appear to start to breakdown lignin and may lead to an effective pretreatment for biofuels production.

ACKNOWLEDGMENTS

REFERENCES CITED

Azadfallah, M., Mirshokraei, S. A., Latibari, A. J., and Parsapajouh, D. (2008). "Analysis of photodegraded lignin on cellulose matrix by means of FTIR spectroscopy and high pressure size exclusion chromatography," *Iranian Polym. J.* 17(1), 73.

Bouchard, J., Methot, M., and Jordan, B. (2006). "The effects of ionizing radiation on the cellulose of wood free paper," *Cellulose* 13(5), 601-610. DOI: 10.1007/s10570-005-9033-0

Colom, X., Carrillo, F., Nogués, F., and Garriga, P. (2003). "Structural analysis of photodegraded wood by means of FTIR spectroscopy," *Polym. Degrad. Stab.* 80(3), 543-549. DOI: 10.1016/S0141-3910(03)00051-X

Despot, R., Harin, H., Rapp, O. A., Brischke, C., Humar, M., Welzbacher, C. R., and Razem, D. (2012). "Changes in selected properties of wood caused by gamma radiation," *in Gamma Radiation,* J. Adrovic (ed.), InTech, Rijeka, Croatia.

Driscoll, M., Stipanovic, A., Winter, W., Cheng, K., Manning, M., Spiese, J., Galloway, R. A., and Cleland, M. R. (2009). "Electron beam irradiation of cellulose," *Radiat. Phys. Chem.* 78(7–8), 539-542. DOI: 10.1016/j.radphyschem.2009.03.080

Fengel, D., and Wegener, G. (1989). *Wood: Chemistry, Ultrastructure, Reactions*, De Gruyter, Germany.

Griffith, W. L., Dorsey, G. F., Harper, D. P., Moschler, W. W., Rials, T. G., and Winstorfer, P. M. (2006). *Electron-Beam Cured Resin Systems for Wood Composites*, ANTEC, Charlotte, NC.

Han, S. O., Cho, D., Park, W. H., and Drzal, L. T. (2006). "Henequen/poly (butylene succinate) biocomposites: Electron beam irradiation effects on henequen fiber and the interfacial properties of biocomposites," *Compos. Interfaces*. 13, 2(3), 231-247.

Hallman, G. J. (2011). "Phytosanitary applications of irradiation," *Compr. Rev. Food Sci. Food Saf.* 10(2), 143-151. DOI: 10.1111/j.1541-4337.2010.00144.x

Hon, D. N. S., and Shang-Tzen, C. (1984). "Surface degradation of wood by ultraviolet light," *J. Polym. Sci. Polym. Chem. Ed.* 22(9), 2227-2241. DOI: 10.1002/pol.1984.170220923

Horvath, B., Peralta, P., Frazier, C., and Peszlen, I. (2011). "Thermal softening of transgenic aspen," *BioResources* 6(2), 2125-2134.

Ivanov, V. S. (1992). *Radiation Chemistry of Polymers*, VSP, The Netherlands.

Joy, D. C. (1995). "A database on electron-solid interactions," *Scanning* 17, 270-275. DOI: 10.1002/sca.4950170501

Kauráková, M., Capeka, P., Sasinkova, V., Wellnerb, N., and Ebringerova, A. (2000). "FT-IR study of plant cell wall model compounds: Pectic polysaccharides and hemicelluloses," *Carbohydr. Polym*. 43(2), 195-203. DOI: 10.1016/S0144-8617(00)00151-X

Khan, A. W., Labrie, J.-P., and Mckeown, J. (1986). "Effect of electron-beam irradiation pretreatment on the enzymatic hydrolysis of softwood," *Biotech. Bioeng.* 28, 1449-1453. DOI: 10.1002/bit.260280921

Kretschmann, D. (2010). "Mechanical properties of wood," in: *Wood Handbook*; General Technical report FPL GTR-190, Madison, WI, Forest Service, Forest Products Laboratory: Ch. 5, 5-1, pp. 5-46.

Mitsui, K., Inagaki, T., and Tsuchikawa, S. (2008). "Monitoring of hydroxyl groups in wood during heat treatment using NIR spectroscopy," *Biomacromol*. 9(1), 286-288. DOI: 10.1021/bm7008069

Labbé, N., Harper, D., Rials, T., and Elder, T. (2006). "Chemical structure of wood charcoal by infrared spectroscopy and multivariate analysis," *J. Ag. Food Chem.* 54, 3492-3497. DOI: 10.1021/jf053062n

Pettersen, R. C. (1984). "The chemical composition of wood," *Adv. Chem. Ser*. 207, 57-126. DOI: 10.1021/ba-1984-0207.ch002

Pruzinec, J., Kadlecik, J., Varga, S., and Pivovarnicek, F. (1981). "Study of the effects of high-energy radiation on cellulose," *Radiochem. Radioanal. Lett*. 49, 395.

Purdy, J. A., Perez, C. A., and Vijayakumar, S. (2012). *Technical Basis of Radiation Therapy*, Springer.

Saeman, J. F., Millett, M. A., and Lawton, E. J. (1952). "Effect of high energy cathode rays on cellulose," *Ind. Eng. Chem*. 44(12), 2848-2852. DOI: 10.1021/ie50516a027

Singh, A. (2001). "Radiation processing of carbon fibre-reinforced advanced composites," *Nucl. Instrum. Methods Phys. Res. Sect. B Beam Interact. Mater. Atoms*. 185(1-4), 50-54.

Song, T. (2005). "Electron beam cured resins for wood composites," Thesis presented for M.S, University of Tennessee, Knoxville.

Sun, N., Das, S., and Frazier, C. (2007). "Dynamic mechanical analysis of dry wood: Linear viscoelastic response region and effects of minor moisture changes," *Holzforschung* 61(1), 28-33. DOI: 10.1515/HF.2007.006

Tsuchikawa, S., and Siesler, H. W. (2003). "Near-infrared spectroscopic monitoring of the diffusion process of deuterium-labeled molecules in wood. Part I: softwood," *Appl. Spectrosc*. 57(6), 667-674. DOI: 10.1366/000370203322005364